Steady-State Phosphorylation of Light-Harvesting Complex II Proteins Preserves Photosystem I under Fluctuating White Light[1][W][OA]

Michele Grieco, Mikko Tikkanen, Virpi Paakkarinen, Saijaliisa Kangasjärvi, and Eva-Mari Aro*

Molecular Plant Biology, Department of Biochemistry and Food Chemistry, University of Turku, FIN–20014 Turku, Finland

According to the "state transitions" theory, the light-harvesting complex II (LHCII) phosphorylation in plant chloroplasts is essential to adjust the relative absorption cross section of photosystem II (PSII) and PSI upon changes in light quality. The role of LHCII phosphorylation upon changes in light intensity is less thoroughly investigated, particularly when changes in light intensity are too fast to allow the phosphorylation/dephosphorylation processes to occur. Here, we demonstrate that the Arabidopsis (*Arabidopsis thaliana*) *stn7* (for state transition7) mutant, devoid of the STN7 kinase and LHCII phosphorylation, shows a growth penalty only under fluctuating white light due to a low amount of PSI. Under constant growth light conditions, *stn7* acquires chloroplast redox homeostasis by increasing the relative amount of PSI centers. Thus, in plant chloroplasts, the steady-state LHCII phosphorylation plays a major role in preserving PSI upon rapid fluctuations in white light intensity. Such protection of PSI results from LHCII phosphorylation-dependent equal distribution of excitation energy to both PSII and PSI from the shared LHCII antenna and occurs in cooperation with nonphotochemical quenching and the proton gradient regulation5-dependent control of electron flow, which are likewise strictly regulated by white light intensity. LHCII phosphorylation is concluded to function both as a stabilizer (in time scales of seconds to minutes) and a dynamic regulator (in time scales from tens of minutes to hours and days) of redox homeostasis in chloroplasts, subject to modifications by both environmental and metabolic cues. Exceeding the capacity of LHCII phosphorylation/dephosphorylation to balance the distribution of excitation energy between PSII and PSI results in readjustment of photosystem stoichiometry.

Plant acclimation to different quantities and qualities of light has been extensively investigated. The light quality experiments have usually concerned the red/blue and far-red light acclimation strategies, which have been closely related to the state transitions and the phosphorylation of the light-harvesting complex II (LHCII) proteins, Lhcb1 and Lhcb2, by the state transition7 (STN7) kinase (Allen, 2003; Bellafiore et al., 2005; Bonardi et al., 2005; Tikkanen et al., 2006; Rochaix, 2007). Such studies on acclimation to different qualities of light have uncovered key mechanisms required for the maintenance of photosynthetic efficiency in dense populations and canopies (Dietzel et al., 2008). However, the role of LHCII phosphorylation under fluctuations in the quantity of white light has been scarcely investigated. Light conditions in natural environments may be very complex with respect to the quantity of white light, which constantly fluctuates both in short- and long-term durations (Smith, 1982; Külheim et al., 2002). Thus, the acclimation strategies to natural environments must concomitantly meet the challenges of both high- and low-light acclimation. Changing cloudiness, for example, would initiate both the high-light and low-light acclimation signals in the time scale of minutes and hours, whereas the movements of leaves in the wind or the rapid movement of clouds would initiate even more frequent light acclimation signals. The kinetics of reversible LHCII phosphorylation is far too slow to cope with rapid environmental changes.

The phosphorylation level of LHCII proteins in the thylakoid membrane is regulated by both the STN7 kinase and the counteracting PPH1/TAP38 phosphatase (Pribil et al., 2010; Shapiguzov et al., 2010). No definite results are available about regulation of the PPH1/TAP38 phosphatase, but the STN7 kinase is strongly under redox regulation (Lemeille et al., 2009) and controls the phosphorylation level of LHCII proteins under varying white light intensities as well as according to chloroplast metabolic cues, as described already decades ago (Fernyhough et al., 1983; Rintamäki et al., 2000; Hou et al., 2003). So far, research on the role of the STN7 kinase and LHCII phosphorylation in the light acclimation of higher plants has heavily focused on reversible LHCII phosphorylation and concomitant

[1] This work was supported by the Academy of Finland (project nos. 118637 to E.-M.A., 260094 to M.T., and 218157 and 130595 to S.K.) and the European Union Marie Curie Initial Training Network – Chloroplast Signaling (project no. GA–215174) for M.G. and E.-M.A.

* Corresponding author; e-mail evaaro@utu.fi.

The author responsible for distribution of materials integral to the findings presented in this article in accordance with the policy described in the Instructions for Authors (www.plantphysiol.org) is: Eva-Mari Aro (evaaro@utu.fi).

[W] The online version of this article contains Web-only data.

[OA] Open Access articles can be viewed online without a subscription.

www.plantphysiol.org/cgi/doi/10.1104/pp.112.206466

state transitions. The state 1-to-state 2 transition, by definition, means the phosphorylation of LHCII proteins, their detachment from PSII in grana membranes, and migration to the stroma membranes to serve in the collection of excitation energy to PSI (Fork and Satoh, 1986; Williams and Allen, 1987; Wollman, 2001; Rochaix, 2007; Kargul and Barber, 2008; Murata, 2009; Lemeille et al., 2010; Minagawa, 2011). Concomitantly, the absorption cross section of PSII decreases and that of PSI increases (Canaani and Malkin, 1984; Malkin et al., 1986; Ruban and Johnson, 2009). Indeed, state transitions have been well documented when different qualities (blue/red and far red) of light, preferentially exciting either PSII or PSI, have been applied.

Different from state transitions, the white light intensity-dependent reversible LHCII phosphorylation does not result in differential excitation of the two photosystems (Tikkanen et al., 2010). Instead, both photosystems remain nearly equally excited independently whether the LHCII proteins are heavily phosphorylated or strongly dephosphorylated. Moreover, it is worth noting that the different qualities of light generally used to induce reversible LHCII phosphorylation and state transitions (blue/red and far-red lights) have usually been of very low intensity (for review, see Haldrup et al., 2001), and apparently, minimal protonation of the lumen takes place under such illumination conditions. Yet another difference between induction of LHCII protein phosphorylation by different qualities of light or different quantities of white light concerns the concomitant induction of PSII core protein phosphorylation. In the former case, the level of PSII core protein phosphorylation follows the phosphorylation pattern of LHCII proteins, whereas under different quantities of white light, the phosphorylation behavior of PSII core and LHCII proteins is the opposite (Tikkanen et al., 2008b).

To gain a more comprehensive understanding of the physiological role of white light-induced changes in LHCII protein phosphorylation, we have integrated Arabidopsis (*Arabidopsis thaliana*) LHCII phosphorylation with other light-dependent regulatory modifications of light harvesting and electron transfer in the thylakoid membrane, which include the nonphotochemical quenching of excitation energy (for review, see Niyogi, 1999; Horton and Ruban, 2005; Barros and Kühlbrandt, 2009; de Bianchi et al., 2010; Jahns and Holzwarth, 2012; Ruban et al., 2012) and the photosynthetic control of electron transfer by the cytochrome b_6f (Cytb6f) complex (Rumberg and Siggel, 1969; Witt, 1979; Tikhonov et al., 1981; Bendall, 1982; Nishio and Whitmarsh, 1993; Joliot and Johnson, 2011; Suorsa et al., 2012; for review, see Foyer et al., 1990, 2012), both strongly dependent on lumenal protonation.

It is demonstrated that the steady-state LHCII phosphorylation is particularly important under rapidly fluctuating light (FL) conditions. This ensures equal energy distribution to both photosystems, prevents the accumulation of electrons in the intersystem electron transfer chain (ETC), eliminates perturbations in chloroplast redox balance, and maintains PSI functionality upon rapid fluctuations in white light intensity.

RESULTS

Phenotypes of Arabidopsis Wild-Type and *stn7* Mutant Plants Grown under Different Light Conditions

In order to investigate the mechanisms that enable the acclimation of Arabidopsis to rapidly changing light intensities, we set up an illumination device in which the intensity of white light fluctuates (FL): low light (60 μmol photons m^{-2} s^{-1}) is interrupted every 5 min by a 1-min-long high-light (600 μmol photons m^{-2} s^{-1}) peak. Plants developed in this condition for their entire life apparently make use of the full flexibility of the photosynthetic machinery in order to acclimate in the best possible way to such a dynamic growth light condition. As controls, we used plants grown under three different constant light intensities: low, moderate, and high light (LL, ML, and HL, respectively). ML plants received roughly an equal number of photons as the FL plants during the 8-h photoperiod.

Different Arabidopsis mutant lines grown under FL and the three different constant light intensities are described in Table I. In addition to the *stn7* single mutant, we also tested other thylakoid mutants for growth under FL, including *stn8*, *stn7 stn8*, *npq4*, *npq4 stn7*, and *npq1*, with known defects in regulation of the LHCII-PSII function (Niyogi et al., 1998, 2005; Bonardi et al., 2005; Vainonen et al., 2005; Frenkel et al., 2007; Tikkanen et al., 2008a). Under FL, all mutant plants lacking the STN7 kinase grew significantly slower compared with the wild type or the *stn8* and *npq* mutants (Fig. 1A; Supplemental Fig. S1). On the contrary, growth under constant LL, ML, and HL did not result in the visual

Table I. *Thylakoid regulatory mutants used in the experiments*

Mutant	Defective Protein Product	Function	Reference
stn7	STN7 kinase	LHCII phosphorylation	Bellafiore et al. (2005); Bonardi et al. (2005); Tikkanen et al. (2006)
stn8	STN8 kinase	PSII core phosphorylation	Bonardi et al. (2005); Vainonen et al. (2005)
stn7 stn8	STN7 and STN8 kinases	LHCII and PSII core phosphorylation	Bonardi et al. (2005)
npq4	PsbS	Feedback deexcitation (NPQ)	Niyogi et al. (2005)
npq4 stn7	STN7 kinase and PsbS	LHCII phosphorylation and feedback deexcitation (NPQ)	Frenkel et al. (2007)
npq1	Violaxanthin deepoxidase	Zeaxanthin-dependent NPQ	Niyogi et al. (1998)

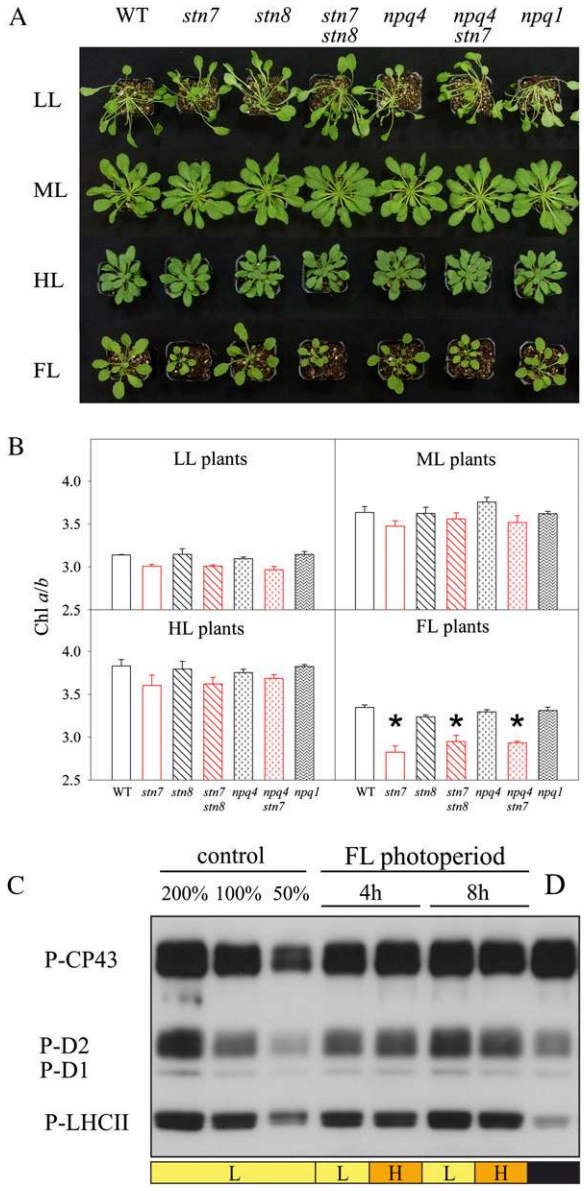

Figure 1. Phenotypes of Arabidopsis wild-type (WT) and mutant plants grown under constant light and FL. A, Visual phenotypes of plants grown under constant LL, ML, and HL white light intensity (50, 130, and 500 μmol photons m^{-2} s^{-1}, respectively) and under FL (i.e. alternation of 5 min of low-intensity white light [60 μmol photons m^{-2} s^{-1}] and 1 min of high-intensity white light [600 μmol photons m^{-2} s^{-1}]) during the 8-h photoperiod. Plants were photographed 8 weeks (LL), 4 weeks (ML), 3 weeks (HL), and 6 weeks (FL) after sowing the seeds. B, The chl *a/b* ratio. Asterisks indicate statistically significant differences between wild-type and *stn7* plants at $P < 0.001$. Values are means ± SD from three independent growth experiments, with five plants each. C, Phosphorylation of thylakoid proteins in wild-type plants during the cyclic phases of fluctuating growth light. Wild-type plants were grown under FL for 8 weeks. Leaf samples were collected at the end of two different cycles of LL (L) and HL (H) phases of FL after 4 and 8 h from the beginning of the 8-h photoperiod and at the end of the dark phase (D). Phosphorylation of thylakoid proteins was determined by immunoblotting with phosphorylated Thr antibody. P-CP43, P-D2, P-D1, and P-LHCII indicate the phosphorylated PSII core proteins CP43, D2, and D1 and the LHCII proteins Lhcb1 and Lhcb2. The immunoblot shown is representative of three independent experiments.

phenotype of the mutants being different from that of the wild type.

Chlorophyll *a/b* (chl *a/b*) ratio was first used as a parameter to monitor the acclimation processes. Under constant growth light conditions, only the *stn7* mutants showed slightly lower values of chl *a/b* ratio compared with the wild type and the other mutants (Fig. 1B). Intriguingly, however, in plants grown under FL, the chl *a/b* ratio was distinctly lower in all the *stn7* mutants than in the wild type or the *stn8* and *npq* mutants. These differences in the chl *a/b* ratio in plants grown under FL suggested modification(s) in the stoichiometry of the main photosynthetic pigment protein complexes.

Importantly, the FL conditions were designed such that the 1-min HL pulse was not long enough to induce changes in the level LHCII protein phosphorylation of wild-type plants (Fig. 1C).

Stoichiometry of Thylakoid Protein Complexes and Extent of Protein Phosphorylation during Light Acclimation

To gain deeper insights into structural modifications of the thylakoid membrane in the absence of STN7, we next focused on wild-type and *stn7* mutant plants grown under constant LL, ML, and HL conditions as well as under FL. Thylakoid pigment protein complexes were solubilized with dodecyl maltoside and separated by large-pore blue-native (lpBN)-PAGE (Järvi et al., 2011) in the first dimension, and then the individual proteins constituting the protein complexes were separated by SDS-PAGE. The gels were first stained with ProQ Diamond, a quantitative dye for phosphoproteins, and then with SYPRO Ruby, a quantitative dye for total proteins. Figure 2A shows the representative one-dimensional and two-dimensional (2-D) gels from thylakoid membranes of the wild type and *stn7* grown under FL. The nomenclature of the protein complexes separated by lpBN-PAGE is based on Järvi et al. (2011), and the identification of the individual proteins is based on Aro et al. (2005). The relative amounts of PSI and PSII, and their respective antennae LHCI and LHCII, were analyzed by spot densitometry from the 2-D gels using representative proteins of the chlorophyll-binding complexes: CP47 and CP43 for PSII, PsaA and PsaB for PSI, Lhcb1 and Lhcb2 for LHCII, and Lhca2 and Lhca3 for LHCI. These data allowed comparison of the ratios of different pigment protein complexes between the wild type and *stn7* on the one hand, and on the other hand they made it possible to analyze the acclimation strategy at the level of pigment protein complexes of both the wild type and *stn7* to different growth light conditions (Fig. 2B).

The *stn7* mutant plants grown under constant LL, ML, and HL showed lower PSII/PSI ratios as compared with the wild type. On the contrary, for plants grown under FL, the opposite result was obtained, the

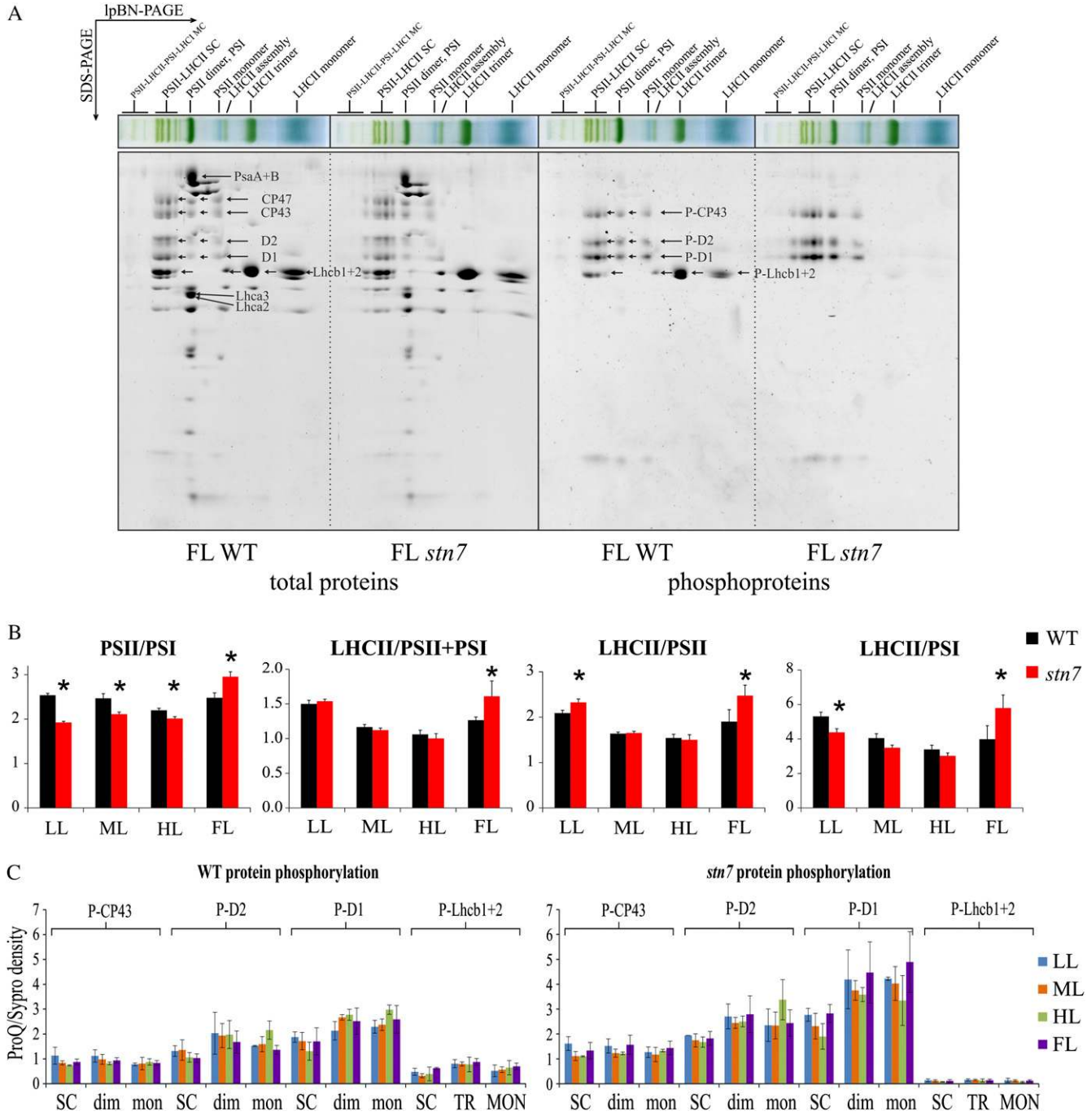

Figure 2. Relative amounts and phosphorylation patterns of photosystems and antennae from wild-type and *stn7* plants grown under LL, ML, HL, and FL conditions. A, 2-D lpBN-PAGE of thylakoid proteins isolated from wild-type and *stn7* mutant plants grown under FL (FL WT and FL *stn7*, respectively). The thylakoid membranes were entirely solubilized by dodecyl maltoside. Every gel was stained both with SYPRO Ruby, a quantitative dye for total proteins, and ProQ Diamond, a quantitative dye for phosphoproteins. The protein spots used for the densitometry are labeled. Proteins were identified based on Aro et al. (2005). MC, Megacomplex; SC, supercomplex. B, Relative amounts of antennae and photosystems in plants grown under LL, ML, HL, and FL. PSII/PSI, PSII/PSI ratio; LHCII/PSII+PSI, light-harvesting complex/photosystems ratio. Data were obtained by spot densitometry of 2-D lpBN gels stained by SYPRO Ruby dye. Asterisks indicate statistically significant differences between wild-type and *stn7* plants at $P < 0.05$. Values are means of three independent experiments ± SD. C, Phosphorylation patterns of PSII (P-CP43, P-D2, P-D1) and LHCII (P-Lhcb1+2) in plants grown under LL, ML, HL, and FL. The protein phosphorylation level was calculated as a ProQ/SYPRO densitometric ratio of 2-D lpBN-PAGE spots. Gels were loaded based on chlorophyll content (8 μg per sample). SC, Supercomplex; dim, PSII dimer; mon, PSII monomer; TRIM, LHCII trimer; MON, LHCII monomer. Values are means of three independent experiments ± SD.

PSII/PSI ratio being clearly higher in the *stn7* mutant than in the wild type (Fig. 2B). In plants developed under constant light, the LHCII/(PSII+PSI) ratio was similar between the wild type and the *stn7* mutant, but the FL growth conditions again resulted in a difference, this ratio being higher in the *stn7* plants compared with the wild type. This result was partially due to a higher LHCII/PSII ratio in the *stn7* mutant plants grown under FL compared with the wild type but was also affected by the remarkably higher LHCII/PSI ratio in the *stn7* mutant plant (Fig. 2B).

Analysis of thylakoid protein phosphorylation in wild-type and *stn7* plants from different growth conditions was performed by normalizing the phospho signal to the amount of the respective protein signal determined from the same gel after staining with ProQ and SYPRO, one after another (Fig. 2C). We first tested whether the phosphorylation level of thylakoid proteins changed in the course of light intensity fluctuations under FL growth conditions. As shown in Figure 1C, fluctuations in light intensity in the minutes time scale did not significantly affect the phosphorylation level of thylakoid proteins. Comparisons of steady-state thylakoid protein phosphorylation between different growth conditions and between wild-type and *stn7* thylakoids were always made between samples run side by side on the same gel. As can be seen from Figure 2C, the relative phosphorylation of the PSII core proteins in the wild type was several times higher than that of the LHCII proteins, and the highest phosphorylation level of LHCII proteins occurred under FL growth conditions. As expected, the LHCII phosphorylation in the *stn7* mutant was negligible. Nevertheless, the steady-state phosphorylation level of the PSII core proteins CP43, D2, and D1 under the light period was higher in the *stn7* mutant than in the wild type under all different growth conditions. This suggests that the *stn7* mutant, in the absence of LHCII protein phosphorylation, generally keeps the plastoquinone/plastoquinol (PQ) pool more reduced compared with the wild type. Neither the PSII core nor the LHCII protein phosphorylation level was drastically affected whether the plants were grown under LL, ML, or HL conditions. Since the phosphorylation of the PSII core proteins by the STN8 kinase is regulated by the redox state of the PQ pool (Tikkanen et al., 2008a), these results suggest that plants achieve a redox balance upon acclimation to different light intensities.

Immunoblot analyses of the wild type and *stn7* grown under ML and FL were performed as a second approach to estimate the relative amounts of representative proteins of the main photosynthetic protein complexes (Fig. 3): PSII (D1), PSI (PsaB), LHCII (Lhcb2), LHCI (Lhca1), and Cytb6f (Cyt f) for linear electron flow; NAD(P)H dehydrogenase (NdhL), PTOX, PGRL1, and proton gradient regulation5 (PGR5) for alternative pathways and regulation of photosynthetic electron flow; ATP synthase (ATPβ) and Rubisco (RbcL) for stromal carbon fixation. Wild-type and *stn7* plants revealed similar changes in photosystem stoichiometry to those observed by 2-D lpBN-PAGE analysis (Fig. 2). The PSII level, revealed by the D1 protein, was only slightly lower in *stn7* compared with the wild type in both ML and FL, whereas no distinct differences were found in the relative amounts of ATP synthase, Cytb6f or NADPH-dehydrogenase (NdhL), PTOX, PGRL1, and PGR5. Rubisco showed some decline in FL growth conditions, but this occurred both in the wild type and *stn7*. Interestingly, a clear difference between *stn7* mutant and wild-type thylakoids from the constant ML growth

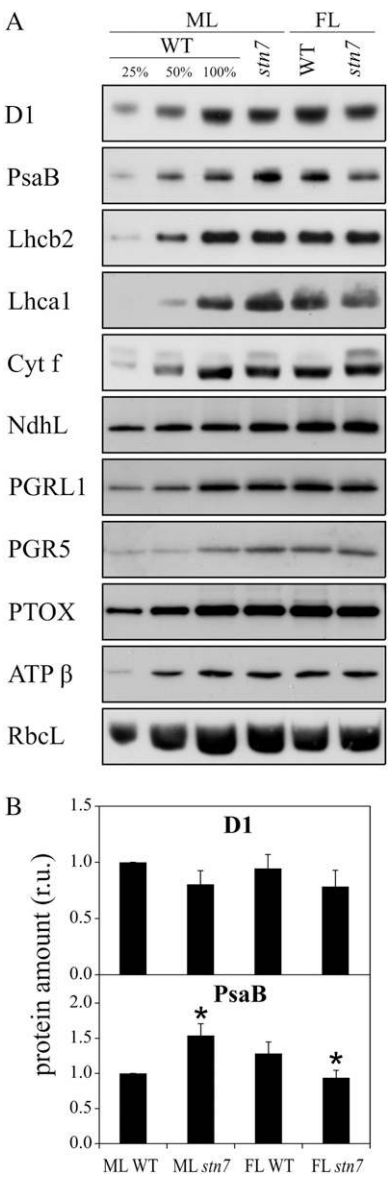

Figure 3. Photosynthetic proteins in wild-type (WT) and *stn7* mutant plants grown under ML and FL. A, Immunoblotting. Gels were loaded based on chlorophyll content (chlorophyll amount varied depending on the primary antibody). B, Densitometry of D1 and PsaB proteins. Asterisks indicate statistically significant differences between wild-type and *stn7* plants at $P < 0.05$. r.u., Relative units of densitometry intensity. Gels are representative of three independent experiments.

condition was a higher relative amount in *stn7* of the PsaB protein, indicative of the content of the PSI centers, as well as of the LHCI antenna (Fig. 3). In sharp contrast to ML growth conditions, under FL growth conditions the amounts of PSI as well as LHCI were substantially lower in the *stn7* mutant than in the wild type, thus corroborating the results obtained from total SYPRO staining experiments (Fig. 2).

To reveal the origin of a substantially lower chl *a/b* ratio of the *stn7* thylakoids from FL-grown plants compared with the wild type, and a minor difference between *stn7* and the wild type under ML conditions, the major chlorophyll protein bands were excised from the one-dimensional lpBN-PAGE, chlorophyll was extracted, and the chl *a/b* ratios of the pigment protein complexes were measured (Supplemental Fig. S2). A minor decrease in chl *a/b* ratio in *stn7* grown under ML as compared with the wild type seemed to be evenly distributed among all antenna and photosystem complexes. The chl *a/b* ratios in FL-grown *stn7* plants also showed a similar pattern as in the wild type, except for the PSII dimer + PSI monomer band, which revealed a lower chl *a/b* ratio in *stn7* than the corresponding band of the wild type or in the ML-grown *stn7* plants. This result is consistent with a low content of PSI centers in *stn7* grown in FL. The fractions of total chlorophyll associated with each pigment protein complex in the wild type and *stn7* under FL and ML are depicted in Supplemental Figure S2.

To further investigate the relative differences in the pigment protein complexes, as described above, the distribution of excitation energy between PSII and PSI was examined by 77 K chlorophyll *a* fluorescence emission spectra, recorded from thylakoids isolated from wild-type and *stn7* mutant plants grown in all four different light conditions (Supplemental Fig. S3A). The PSII/PSI fluorescence ratios calculated from the spectra are shown in Supplemental Figure S3B. In all growth conditions, the *stn7* mutant showed a higher value compared with the wild type. As expected, the lack of LHCII phosphorylation favored the excitation of PSII. However, the difference in PSII/PSI fluorescence ratio between wild-type and *stn7* plants was remarkably higher in FL compared with the differences observed in constant growth light conditions ($P < 0.01$). This observation confirmed that the PSII/PSI ratio increased in *stn7* grown in FL and, moreover, indicated that such stoichiometric change greatly favors the excitation of PSII.

Functional Properties of Wild-Type and *stn7* Thylakoids upon Acclimation to FL

Functional consequences of the modifications in the amounts of thylakoid protein complexes, which on the one hand led to the acclimation of the *stn7* mutant to constant growth light conditions but on the other hand resulted in impaired growth of *stn7* under FL, were addressed next. The first functional parameter to be addressed was the Q_A redox state, which is an indicator of the redox balance between PSII and PSI and hence describes the flow of electrons in the ETC. The Q_A redox state is commonly measured by the $1\text{-}q_P$ and $1\text{-}q_L$ chlorophyll fluorescence parameters, which estimate the fraction of closed PSII reaction centers, based on the puddle and the lake models, respectively, in steady-state conditions (Dietz et al., 1985; Weis and Berry, 1987; Gray et al., 1996; Hüner et al., 1996; Kramer et al., 2004). However, during the HL phases of FL and in the first half of LL phases, the steady-state condition was not reached. Actually, the aim of using HL pulses was to disturb the steady state in order to challenge the dynamic responses of photosynthetic mechanisms. Therefore, as an indicator of the Q_A redox state, we used the chlorophyll *a* fluorescence yield values under actinic light normalized to the maximal fluorescence F_m (the F'/F_m parameter). Although F'/F_m is not linearly correlated to $[Q_A^-]$ due to the antenna connectivity (Joliot and Joliot, 1964; Lavergne and Trissl, 1995), we used this parameter as a semiquantitative estimation of the reduction level of Q_A (denoted as "relative Q_A redox state") to indicate relative changes under non-steady-state conditions.

Fluorescence was first monitored from the wild type and the *stn7*, *stn8*, *stn7 stn8*, *npq4*, *npq4 stn7*, and *npq1* mutants grown both in ML and FL conditions by mimicking the same illumination program as during the growth under FL (actinic fluctuating light [AFL] = 5 min of low green light and 1 min of high green light repeating the entire measuring period) using the JTS-10 spectrofluorometer (BioLogic; Fig. 4). The first low-intensity period of the three FL cycles was different from the other cycles and gave information on the activation of photosynthesis after the dark incubation, while all the following ones showed a cyclic repetition during the AFL experiment (only two such cycles are shown in Fig. 4). The Q_A reduction showed a similar low steady-state value upon low-illumination phases of AFL in all *stn7* mutants grown under ML and in the wild type grown in both ML and FL. However, in FL-grown *stn7* plants, the Q_A reduction level reached a much higher value during the low-illumination phase of AFL, indicating an imbalance in the excitation of PSII and PSI, in favor of PSII, and resulting in the accumulation of electrons in the intersystem ETC. Since the F'/F_m parameter in the second half of the low-light illumination phases of AFL reached a steady-state value, it can be used also as an indicator of the PQ pool redox state.

These results raised the question of whether the observed redox unbalance was related to the lack of STN7 kinase itself or rather to the lack of LHCII docking to PSI. To this end, we analyzed the *psal* mutant plants, which revealed a similar visual phenotype as the *stn7* plants when grown under FL conditions (Supplemental Fig. S4A) and have previously been shown to be impaired in phosphorylated LHCII binding to PSI and consequently also in state transitions (Lunde et al., 2000). The same measurements as shown in Figure 4 were carried out on *psal* mutant plants, grown in constant ML and in FL conditions (Supplemental Fig. S4B).

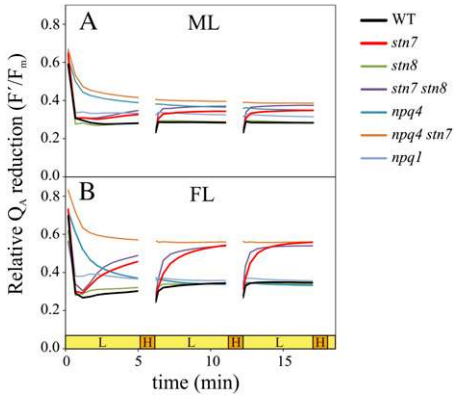

Figure 4. Relative Q_A reduction in wild-type (WT) and *stn7*, *stn8*, *stn7 stn8*, *npq4*, *npq4 stn7*, and *npq1* mutant plants during the LL phases of FL. The relative Q_A reduction was measured by the chlorophyll fluorescence parameter F'/F_m, in plants grown in ML (A) and FL (B) conditions, under actinic light that mimicked the FL growth condition (AFL). Detached leaves were incubated in darkness for 15 min before measurements. L, LL phase of AFL; H, HL phase of AFL. No measuring points were detected during H.

Functional analysis of the PQ pool redox state under AFL revealed that the lack of the PsaL protein results in a significant increase in the PQ pool reduction state during the LL phases of AFL in plants grown under FL ($P < 0.01$). In ML growth conditions, on the contrary, the *psal* mutant showed a full compensation of mutation. These results follow the same trends observed in the *stn7* plants, although in a less drastic way. This is apparently due to the fact that the *psal* mutant is still able to perform state transitions equal to about 30% of the wild type (Lunde et al., 2000). The similarity of *psal* and *stn7* mutant phenotypes under FL suggested that the STN7 kinase-induced LHCII phosphorylation is a key factor for redox balancing under FL, not the STN7 kinase per se. It was concluded that the capacity to maintain the dynamics of the light-harvesting apparatus and balanced excitation of both PSII and PSI, despite fluctuations in the light intensity, determines the success of growth under strongly FL conditions.

Fluctuating growth light-mimicking fluorescence experiments were repeated with FL-grown wild-type and mutant plants using a Dual-PAM (for pulse amplitude modulation) spectrofluorometer, which enables simultaneous measurements of both PSII and PSI functionality. Four photosynthetic parameters were measured: (1) the reduction level of Q_A (F'/F_m); (2) the reduction level of P700 reaction centers; (3) the nonphotochemical quenching of excitation energy (NPQ); and (4) the PSI acceptor side limitation [Y(NA); Fig. 5].

The F'/F_m of wild-type leaves slightly increased in the beginning of the low-intensity light period of AFL and then stabilized to a low steady-state level. In the *stn7* and *stn7 stn8* mutants, the F'/F_m in the beginning of the low-intensity light period had almost the same value as the wild type but then increased greatly and stayed high during the entire LL illumination phase of AFL. In the *npq4 stn7* mutant, F'/F_m was high as well and remained at this high level for the entire duration of AFL. Indeed, all plants lacking the STN7 kinase showed nearly similar steady state of F'/F_m, which reached a level much higher than that in the wild type and the other mutants (Fig. 5A). This result thus confirmed the high reduction level of the PQ pool in all *stn7* mutants when grown under FL conditions.

The behavior of PSI and NPQ under AFL was recorded next. During the LL illumination period of AFL, the P700 reaction centers were fully reduced (Fig. 5B), and NPQ was very low in both the wild type and the *stn7* mutant (Fig. 5C). Upon switching on the 1-min HL pulse of AFL, NPQ was rapidly induced in the wild type. The PSI reaction centers were rapidly oxidized in the wild type upon the HL pulse (Fig. 5B). Similar trends were monitored in the *stn7* mutant during the HL period of AFL. Distinctively, however, in *stn7* mutants, PSI was oxidized more slowly and to a lesser extent than in the wild type. NPQ was similarly low during the LL phase in all plants (Fig. 5C). Upon the HL phase, the wild type as well as the *stn8* and *stn7* mutants showed

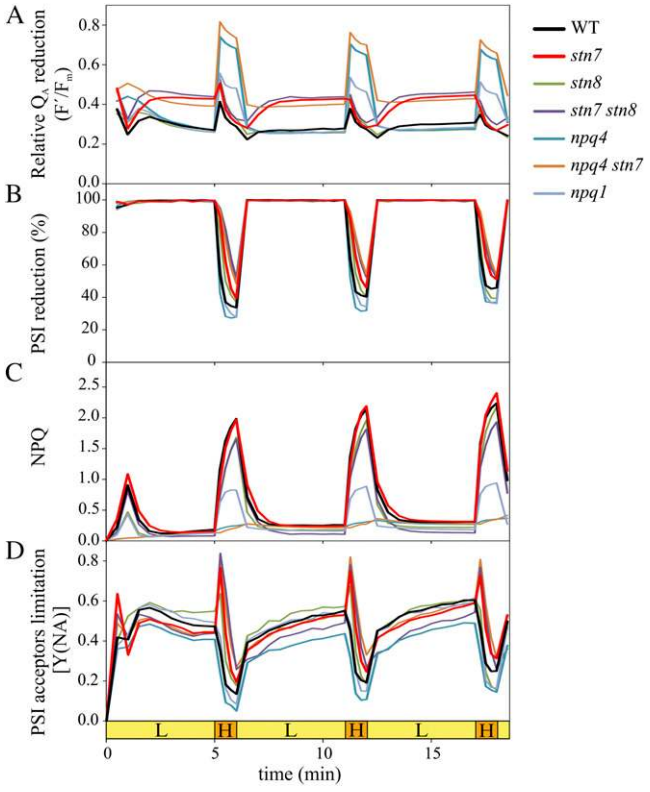

Figure 5. Photosynthetic parameters of wild-type (WT) and *stn7*, *stn8*, *stn7 stn8*, *npq4*, *npq4 stn7*, and *npq1* mutant plants grown in FL conditions. Measurements were performed under actinic light that mimicked the FL growth condition (AFL). A, Relative Q_A reduction measured by the chlorophyll fluorescence parameter F'/F_m. B, PSI reduction monitored as a percentage of reduced P700 reaction centers. C, NPQ. D, Y(NA). Detached leaves were incubated in darkness for 15 min before measurements. Values are means from three independent experiments. L, LL phase of AFL; H, HL phase of AFL.

very similar development of NPQ, while it was low in *npq1* and nearly nonexistent in *npq4* and *npq4 stn7*.

The Y(NA) parameter was measured to estimate the fraction of P700 reaction centers that are closed due to acceptor side limitation (i.e. due to the reduction of the first electron acceptors of PSI; Klughammer and Schreiber, 1994). A striking feature of all plants lacking the STN7 kinase was a clearly higher PSI acceptor limitation value during the HL phases of AFL compared with the other plants (Fig. 5D).

Comparison in the *stn7* mutant plants of the behavior of F'/F_m and NPQ (Fig. 5, A and C) revealed that the strongly reduced PQ pool during LL periods was gradually oxidized to the wild-type level when NPQ became induced upon subsequent HL pulse. This indicates that the induction of NPQ helps in restoring the redox balance of the PQ pool altered by the lack of LHCII phosphorylation. This compensation, however, is not operational under low quenching states.

PSI Modifications in the Acclimation Process of the *stn7* Mutants

Based on results above, it is conceivable that upon growth under constant light intensities, the lack of STN7 is compensated by increasing the amount of PSI complexes (Figs. 2 and 3). Increase in PSI, in turn, maintained a relatively low reduction level of the PQ pool observed during the measurements under AFL. Such adjustment of PSI centers, however, did not occur in *stn7* grown under FL. On the contrary, the abundance of PSI centers in *stn7* diminished under FL growth conditions. This prompted us to take a closer look at the role of PSI in the light acclimation process of the *stn7* mutants.

A method was set up to correlate the amount of PSI with the structural and functional alterations of *stn7* plants described above by measuring the oxidation level of the P700 reaction centers. A saturating pulse (SP) was given to a leaf disc during far-red light illumination, allowing the calculation of the maximal oxidizable P700 centers, called P_m (Klughammer and Schreiber, 1994), being proportional to the total amount of PSI (Supplemental Fig. S5). The P_m values were normalized to the leaf disc chlorophyll content (P_m μg^{-1} chlorophyll). In these same measurements, prior to flashing the SP, the P700 oxidation level reached a plateau during the far-red light illumination (720-nm wavelength), which, however, did not result in the full oxidization of PSI centers. Consequently, the redox steady state during the far-red light illumination implied the presence of an electron flow that partially reduced intersystem ETC and also PSI. The difference between the value of the plateau and P_m was normalized against the P_m value, giving the parameter $\Delta P/P_m$, proportional to the reduction level of the ETC. The possible sources of electrons maintaining the plateau level of P700 oxidation upon far-red illumination include the excitation of PSII at 720-nm light and the cyclic electron flow around PSI. Since no significant differences were observed in the amount of cyclic electron flow complexes (Fig. 3) or in the extent of cyclic electron flow (Supplemental Fig. S6) between the wild type and the *stn7* mutant, we attributed the source of this electron flow to PSII. Therefore, in this specific case of comparison of the wild type and *stn7*, the $\Delta P/P_m$ parameter can be used to estimate the redox balance between PSII and PSI (intersystem redox balance; for details on the method, see "Materials and Methods" and Supplemental Fig. S5).

The two parameters, P_m μg^{-1} chlorophyll and $\Delta P/P_m$, were plotted against the chl *a/b* ratio, the simplest parameter used above to monitor the acclimation processes (Fig. 1B). The results from five different experiments with wild-type and *stn7* sets of plants (six plants in each experiment) grown under ML and FL are shown in Figure 6. The *stn7* mutants grown under constant ML conditions showed a similar pattern to the wild type (Fig. 6, A and C). Both the amount of PSI (P_m μg^{-1} chlorophyll) and the $\Delta P/P_m$ parameter were stable despite clear differences in the chl *a/b* ratio of individual plants from different experiments. Wild-type plants grown under FL conditions behaved similarly to wild-type plants grown under continuous ML conditions (Fig. 6). The *stn7* mutant grown under FL behaved very differently from wild-type plants and from the *stn7* mutant grown under constant ML conditions. First, the amount of PSI (P_m μg^{-1} chlorophyll) appeared to be directly proportional to the chl *a/b* ratio in FL-grown *stn7* mutants (Fig. 6B). Indeed, the lower the chl *a/b* ratio, the smaller was the PSI content in the *stn7* mutant leaves upon growth under FL conditions. Second, the $\Delta P/P_m$ parameter, which describes the reduction level of the ETC, was in the *stn7* mutant grown under FL conditions inversely proportional to the chl *a/b* ratio (Fig. 6D) and thus also to the amount of PSI. It is worth noting that every single set of plants grown under FL (grown at different dates) showed a very characteristic and reproducible pattern: wild-type individuals clustered together, showing very similar values of chl *a/b*, P_m μg^{-1} chlorophyll, and $\Delta P/P_m$, whereas in the *stn7* plants, the chl *a/b* ratio was linearly related to variable amounts of PSI ($r^2 = 0.87 \pm 0.09$) and the $\Delta P/P_m$ parameter values ($r^2 = 0.88 \pm 0.08$). In *stn7* plants grown in FL, $\Delta P/P_m$ was linearly correlated to P_m μg^{-1} chlorophyll ($r^2 = 0.90 \pm 0.03$), indicating that the lower the amount of PSI, the higher is the intersystem redox unbalance (Supplemental Fig. S5). Wild-type and *stn7* plants from the four different growth light conditions (constant LL, ML, and HL as well as FL), except for the FL-grown *stn7* mutants, possessed a rather similar and low value of $\Delta P/P_m$, ranging from 0.2 to 0.3, whereas in the FL-grown *stn7* mutants, the $\Delta P/P_m$ parameter was generally higher and greatly variable (Fig. 6, C and D; results from LL- and HL-grown plants are shown in Supplemental Fig. S7). This provides further evidence that the STN7 kinase ensures functional flexibility of the thylakoid membrane, allowing the maintenance of optimal redox balance between PSII and PSI despite changing light

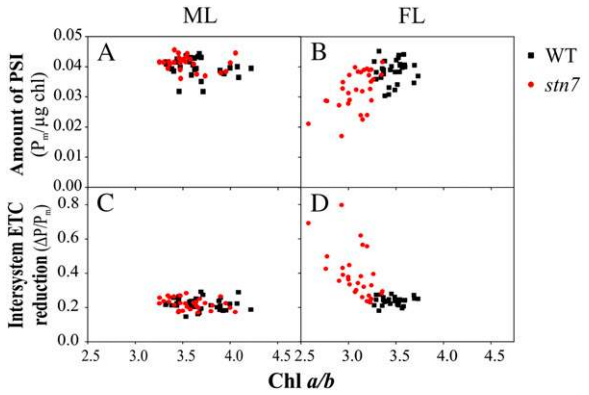

Figure 6. Amount of PSI and the reduction state of intersystem ETC, plotted against chl *a/b* ratio, in wild-type (WT) and *stn7* mutant plants grown under ML and FL. A and B, The amount of PSI (measured as the P_m signal and normalized to chlorophyll content) plotted against chl *a/b* ratio in leaf discs from plants in ML (A) and FL (B) growth conditions. C and D, The state of intersystem ETC reduction (measured as $\Delta P/P_m$; Supplemental Fig. S5A) plotted against chl *a/b* ratio in ML (C) and FL (D) growth conditions from the same leaf discs used in A and B, respectively.

intensities and noticeable structural variations in the photosynthetic apparatus. These data together with the structural analyses above provide strong evidence that the low amount of PSI in the *stn7* mutant results in impaired growth under FL as compared with the wild type.

DISCUSSION

Light acclimation of the photosynthetic apparatus is likely to follow the signals originating in the photosynthetic machinery itself. It is clear both from our experiments here (Figs. 4 and 5A) and from reports published earlier (Bailey et al., 2004; Miyake et al., 2009) that the successful acclimation of plants to changing light environments relates to the capacity of chloroplasts to keep the PQ pool largely oxidized also in the new light environment of both short- and long-term durations. A minimum of three different mechanisms controlling the linear electron transfer and chloroplast redox harmony have been identified so far. (1) The photosystem II subunit S protein and xanthophyll-dependent NPQ (for review, see Niyogi, 1999; Horton and Ruban, 2005; Demmig-Adams and Adams, 2006) is the mechanism that senses the energetic state of the photosynthetic machinery from the extent of lumenal protonation and quenches the excess excitation energy accordingly, affecting not only the redox state of the PQ pool but also the stromal side of PSI. (2) The STN7 kinase also senses the chloroplast redox state both in ETC and on the reducing side of PSI (Rintamäki et al., 2000) and via phosphorylated LHCII proteins balances the effects of NPQ concerning both photosystems, thus enabling the maintenance of excitation and redox balance upon changes in the efficiency of light harvesting (Bellafiore et al., 2005; Tikkanen et al., 2008b, 2010). Indeed, these two mechanisms are not independent but function in close cooperation (Tikkanen et al., 2011). (3) The dynamic "photosynthetic control" of linear electron transfer via the Cytb6f complex between PSII and PSI, according to lumenal protonation, is yet another mechanism that plays a vital role in preventing strong redox fluctuations in ETC (Hope, 1993; Joliot and Johnson, 2011; Suorsa et al., 2012).

Using the mutants of both LHCII protein phosphorylation (*stn7* mutants) and NPQ (*npq1* and *npq4*) as well as various double mutants, we addressed the strategies of both the short- and long-term acclimation of Arabidopsis to constant and fluctuating white light conditions. The stunted growth phenotype (Fig. 1A; Supplemental Fig. S1) and low chl *a/b* ratio (Fig. 1B) were properties of all *stn7* mutants (*stn7*, *npq4 stn7*, and *stn7 stn8*) but only when grown under FL, while the wild type or the *npq* mutants did not reveal distinct differences in the visual phenotype or chl *a/b* ratio upon growth under any of the light conditions applied here (Fig. 1; Supplemental Fig. S1). Success in acclimation to natural fluctuating growth light is dependent both on the steady-state LHCII phosphorylation and its dynamic regulation via the STN7 kinase and PPH1/TAP38 phosphatase activities.

Steady-State LHCII Phosphorylation Preserves PSI upon Rapid Fluctuations of White Light Intensity

The molecular background behind the distinct visual phenotype of *stn7* upon growth under FL (Fig. 1; Bellafiore et al., 2005; Tikkanen et al., 2010) has remained elusive. Actually, depending on the strength of light gradients under fluctuating growth light conditions, a repertoire of *stn7* growth phenotypes, from invisible to very slow growth with chlorotic lesions, can be induced. To reveal the primary factors that lead to the *stn7* phenotype, we first attempted to distinguish whether they result from the lack of STN7-induced LHCII phosphorylation and subsequent perturbations in the regulation of redox homeostasis in chloroplasts or from the lack of the STN7 kinase as a putative retrograde signaling component. To this end, the *psal* mutant of Arabidopsis, which has an active STN7 kinase and LHCII phosphorylation but lacks the energy transfer from phosphorylated LHCII to PSI (Lunde et al., 2000), was analyzed. It revealed a similar phenotype and redox unbalance to the *stn7* mutant under FL growth conditions (Supplemental Fig. S4). These facts provide evidence that the *stn7* phenotype is primarily caused by the excitation and redox unbalance, not by a lack of any unknown phosphorylation-dependent signaling cascade mediated by the STN7 kinase.

As to the mechanism causing the stunted phenotype of *stn7*, it was striking to find out that the FL-grown *stn7* mutant has a high PSII-to-PSI ratio (Figs. 2, 3, and 6; Supplemental Fig. S3). Indeed, this is opposite to the strategy of the *stn7* mutant to increase PSI centers for successful growth under constant light. Thus, either

the HL pulse under FL growth conditions disturbs the redox-based signaling strategy for enhanced synthesis of PSI or the specific damage of PSI under FL causes the *stn7* growth phenotype. Dissecting these two possibilities required a more detailed analysis of the redox behavior in chloroplasts under FL.

Under LL periods, the efficiency of excitation energy transfer to photosystems is at the maximum, and under HL periods, it is at the minimum, as regulated by NPQ (Fig. 7). NPQ thus buffers the effects of changing light intensity on the redox state of the thylakoid membrane. Nonetheless, this occurs successfully only when both photosystems are equally excited and, thus, under a low quenching state, requires LHCII phosphorylation that enables redox balance between the PQ pool and the stromal side of PSI (Rintamäki et al., 2000; Figs. 4–6). On the contrary, in the absence of LHCII phosphorylation (the *stn7* mutants; Fig. 7), the high efficiency of LHCII at LL intensity preferentially excites PSII as compared with PSI, leading to a concomitant strong reduction of the PQ pool but a low reduction state of the PSI stromal side (Figs. 4–7). Shift of *stn7* from LL to HL induces NPQ (Fig. 7), which leads to rapid oxidation of the "overreduced" PQ pool and a concomitant reduction of PSI stromal side electron acceptors. Indeed, the fluctuations between the nonquenched and quenched states in the absence of the STN7 kinase lead to strong short-term changes in the redox state of the PQ pool (Figs. 4B and 5A).

In theory, the unbalanced redox state of the PQ pool could disturb the signaling cascades for enhanced PSI synthesis potentially initiated from the PQ pool (Pfannschmidt et al., 1999; Fernández and Strand, 2008) and thereby lead to a stunted phenotype of *stn7*. Nonetheless, the *stn7 npq4* double mutant shows a high reduction level of ETC both in LL and HL phases of FL (Fig. 5A), yet it has the *stn7* FL growth phenotype. Accordingly, the most likely reason behind the scarcity of PSI centers in the *stn7* mutants grown under FL conditions is their enhanced rate of damage and degradation due to unbalanced excitation energy distribution and electron transfer in the absence of LHCII phosphorylation.

To further investigate this option, we searched for common features for the *stn7* single mutant and *stn7 npq4* double mutants that could lead to damage of PSI. A striking feature of both mutants is the deficiency in oxidation of P700 due to an acceptor side limitation of PSI upon the HL phase of fluctuating growth light, as indicated by the measurements under AFL (Fig. 5, B and D). In general, under HL, the protonation of the lumen not only induces NPQ but also regulates electron transfer via the Cytb6f complex (Rumberg and Siggel, 1969; Witt, 1979; Tikhonov et al., 1981; Bendall, 1982; Nishio and Whitmarsh, 1993; for review see Foyer et al., 1990, 2012). Control via the Cytb6f complex particularly slows down the reduction of the plastocyanin (PC) pool (Eberhard et al., 2008), and it was recently shown that the absence of this central mechanism in the *pgr5* mutant has hazardous consequences on PSI (Joliot and Johnson, 2011; Suorsa et al., 2012). Do the *stn7* mutants fail in the control of electron flow via the Cytb6f complex and thereby induce damage of PSI as in *pgr5* (Suorsa et al., 2012)? Under the LL phases of FL growth, the lumen is only poorly protonated; consequently, there is no control of electron flow by NPQ or the Cytb6f complex in the wild type or the *stn7* mutants.

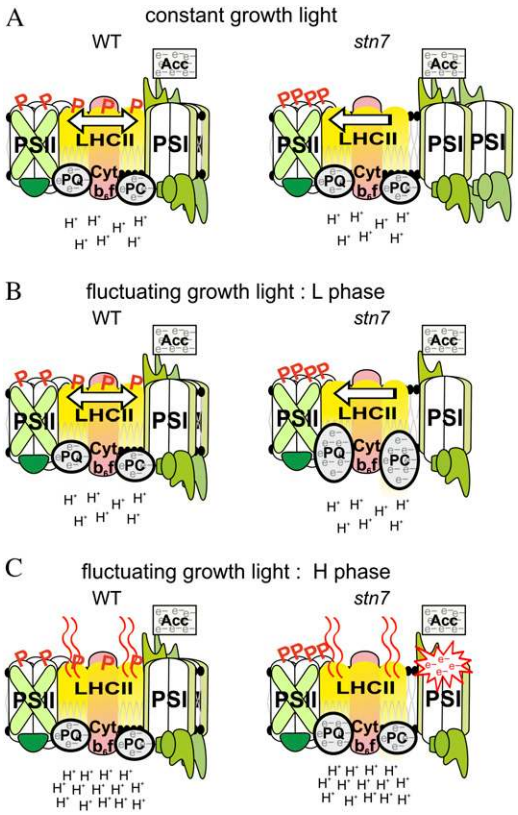

Figure 7. Model of the interplay between LHCII phosphorylation, the photosynthetic control of electron transfer by Cytb6f, and NPQ in wild-type (WT) and *stn7* plants in constant growth light conditions and in LL and HL phases of FL. A, Steady-state constant growth light conditions. In the wild type, LHCII is phosphorylated, protonation of lumen is low, and NPQ and the photosynthetic control of electron transfer by Cytb6f are not induced, ensuring fluent electron flow and redox harmony. In *stn7*, redox harmony is achieved by increasing the amount of PSI centers. B, LL phase of FL. In the wild type, redox harmony is achieved as under steady-state conditions. In *stn7*, when NPQ and the photosynthetic control of Cytb6f are not induced, excess electrons are accumulated in the entire ETC. C, HL phase of FL. In the wild type, the activity of PSII is slowed down by NPQ, preventing the reduction of the PQ pool, and the control of the Cytb6f complex has a similar effect on the PC pool. In *stn7*, a shift to the HL phase provides energy to PSI to oxidize the overreduced ETC. Photosynthetic control of Cytb6f hinders the electron transfer from PQ but does not affect the rapid oxidation of the PC pool. A burst of electrons from overreduced PC damages PSI. Since PSI repair is almost nonexisting, this results in a loss of PSI centers, opposite to constant growth light conditions, where *stn7* increases the amount of PSI centers. Red P denotes protein phosphorylation. Arrows indicate energy transfer. Wavy lines indicate LHCII heat dissipation. The sizes of the circles represent the reduction states of the PQ and PC pools. Acc, Capacity of stromal electron acceptors.

LHCII collects photons in its full efficiency, and in the wild type the intersystem ETC remains mostly oxidized. This balance in the wild type keeps LHCII phosphorylated and both photosystems equally excited. Moreover, the reducing stromal side of PSI in the wild type can easily cope with the slow incoming electron flow (Fig. 5D). The situation with the *stn7* mutants, however, is different, and PSII becomes overexcited as compared with PSI due to the lack of LHCII phosphorylation (Figs. 4 and 5). PSI simply cannot oxidize the intersystem ETC in the lack of enough excitation energy at low illumination phases. Indeed, a high reduction state of the ETC is a common and unique feature for both the *stn7* and *stn7 npq4* mutants under low illumination phases of FL.

In general, the overreduction of the intersystem ETC (PQ pool and PC pool) is not dangerous for PSI. Nevertheless, when the LL phase is followed by a HL phase (Fig. 7), a rapid oxidation of the highly reduced intersystem ETC (mainly the PC pool) in the *stn7* mutants exceeds the capacity of immediate PSI electron acceptors, as indicated by the PSI acceptor side limitation in these mutants (Fig. 5D). Such an excess of electrons has the potential to damage PSI. Indeed, it seems that the mechanism behind the PSI phenotype of the *stn7* mutants results from a sudden burst of electrons accumulated in ETC toward the acceptor side of PSI upon a shift from LL to HL phase of the fluctuating growth light. It is well known that excess electrons are hazardous to the iron-sulfur clusters of PSI (Sonoike et al., 1995). We have recently shown that the protection of PSI from photodamage upon a shift from LL to HL needs a PGR5-dependent mechanism that controls the speed of intersystem electron transfer via the Cytb6f complex under the HL phase (Suorsa et al., 2012). Here, we provide evidence that the excitation balance between PSII and PSI, provided by the STN7 kinase and steady-state LHCII protein phosphorylation, is required to prevent an accumulation of excess electrons in the PC pool under the LL illumination phase. As a consequence of electron accumulation in the PC pool, switching on the HL phase suddenly supplies PSI with enough excitation energy to transfer the excess of electrons from the PC pool to PSI acceptors, causing an electron burst that damages PSI, possibly the iron-sulfur clusters.

The *stn7* Mutant Acclimates to Different Constant Light Intensities by Decreasing the PSII-to-PSI ratio

When changes in white light intensity occur in the time scale of hours, it is likely that the first attempt to balance the redox state of ETC originates from reversible phosphorylation of LHCII. Under constant white light conditions, the extent of LHCII phosphorylation is not at the maximum level. By the interplay between the STN7 kinase and the PPH1/TAP38 phosphatase, upon decrease in light intensity, enhanced phosphorylation occurs, whereas strong dephosphorylation takes place upon increase in light intensity as well as in strongly reduced light intensity (Rintamäki et al., 1997). Thus, the redox unbalances are sensed and transiently corrected by modulations of the level of LHCII protein phosphorylation. Nevertheless, the wild-type plants grown under LL, ML, or HL conditions serve as an example of the fact that the phosphorylation of LHCII proteins eventually reaches a steady-state level that is rather similar irrespective of the light intensity (Fig. 2C). If the changes in light intensity are long lasting and drastic enough, signals for readjustment of the photosynthetic machinery are initiated in order to meet the challenges of the new environment. The fact that the absence of the STN7 kinase causes light intensity-dependent redox unbalance between the intersystem ETC and the PSI stromal side makes the *stn7* mutant an excellent tool to elucidate the roles of the PQ pool and the PSI acceptor side in regulation of the stoichiometry of various components of the photosynthetic machinery.

As shown above, the absence of the STN7 kinase leads to a strong reduction of the PQ pool upon short-term fluctuations in white light intensity. In the long term, the *stn7* mutant compensates this unbalance and shows an oxidized PQ pool at all different constant light conditions. Intriguingly, such compensation does not occur by decreasing the amount of LHCII. Instead, the *stn7* mutant decreases the PSII-to-PSI ratio, which helps in keeping the PQ pool more oxidized. Such regulation strongly suggests, in accordance with previous studies on acclimation to changes in light quality (Pfannschmidt et al., 1999; Tullberg et al., 2000), that the signal(s) for adjusting the relative amounts of the PSII and PSI complexes are triggered by the redox state of the PQ pool (Supplemental Fig. S8).

Nevertheless, it has been unambiguously documented that the size of the LHCII antenna increases upon long-term decrease in the light intensity (Leong and Anderson, 1984; Yang et al., 1998; Bailey et al., 2001). Both the wild type and the *stn7* kinase mutants show rather similar long-term regulation of the LHCII antenna size. Yet, the *stn7* mutant increases the LHCII antenna size under limiting growth light even more than the wild type (Fig. 2), and this occurs despite a much higher reduction level of the PQ pool as compared with the wild type (Figs. 4B, 5A, and 6D). Thus, our results with the *stn7* mutant provide evidence that the actual signal for regulation of the LHCII antenna size originates from the redox state of components on the acceptor side of PSI (Supplemental Fig. S8). Manipulation of the redox state of these two compartments, the ETC and the stroma, in wild-type Arabidopsis has also earlier led us to conclude that the redox compounds (or metabolites) in the stroma are crucial in regulation of the LHCII antenna size (Walters, 2005; Piippo et al., 2006).

In summary, comparison of the acclimation strategies of the wild type and *stn7* with different constant light intensities lead to two important conclusions regarding the initiation or triggering of the retrograde signaling cascades for the adjustment of thylakoid composition. First, the PQ pool redox state provides

signals, by a yet unknown mechanism(s), to the chloroplast and nuclear genomes to initiate long-term acclimation to modulate the relative amounts of the PSII and PSI core complexes according to environmental and metabolic cues. This conclusion is in line with experiments applying different qualities of growth light on mustard (*Sinapis alba*; Pfannschmidt et al., 1999). Second, the increase in the size of the LHCII antenna is regulated by signals originating from the acceptor side of PSI when the chloroplast redox compounds in the stroma are highly oxidized (Supplemental Fig. S8).

CONCLUSION

The STN7 kinase-dependent phosphorylation of LHCII is essential to maintain redox stability in chloroplast under fluctuating intensities of white light. Steady-state LHCII phosphorylation, in cooperation with NPQ- and PGR5-dependent control of electron flow, maintains the functionality of PSI and is crucial for plants to cope with rapid changes in light intensity, for example, with the sun flecks in natural environments. Long-lasting redox changes in ETC are dynamically reflected at the level of LHCII phosphorylation, which then transiently helps in acclimation to a new light environment. Thus, in the very short run, the excitation and redox balance provided by steady-state phosphorylation of LHCII is essential to preserve PSI. In the longer run, reversible LHCII phosphorylation allows a smooth transition phase before the establishment of a new stoichiometry between PSII and PSI and the reestablishment of the steady-state LHCII phosphorylation level. Redox signals for the adjustment of photosystem stoichiometry initiate from the ETC, whereas the signals for LHCII accumulation result from the oxidation of redox components on the reducing side of PSI in the chloroplast stroma.

MATERIALS AND METHODS

Growth of Plants

Wild-type Arabidopsis (*Arabidopsis thaliana*) ecotype Columbia and the *stn7* (Bellafiore et al., 2005), *stn8* (Bonardi et al., 2005), *stn7 stn8* (Bonardi et al., 2005), *npq4* (Niyogi et al., 2005), *npq4 stn7* (Frenkel et al., 2007), and *npq1* (Niyogi et al., 1998) mutant plants were grown in a phytotron at 23°C, relative humidity of 60%, and 8-h photoperiod under three constant white light intensities: LL (50 μmol photons m^{-2} s^{-1}), ML (130 μmol photons m^{-2} s^{-1}), and HL (500 μmol photons m^{-2} s^{-1}). The FL condition consisted of alternations of 5 min of LL (60 μmol photons m^{-2} s^{-1}) and 1 min of HL (600 μmol photons m^{-2} s^{-1}), provided by an automatic shading system, during the 8-h photoperiod. The total number of photons at the FL growth condition corresponded to that of the constant ML growth condition. OSRAM PowerStar HQIT 400/D Metal Halide Lamps served as the light source. Mature rosette leaves from 3-week-old (HL), 4-week-old (ML), and 8-week-old (LL and FL) plants were used for the experiments. From FL, leaves were collected at the end of the LL period. The 1-min HL period upon FL illumination was not long enough to change the phosphorylation of thylakoid proteins.

Chlorophyll Content Measurements

Chlorophyll amount and chl *a*/*b* ratio in leaves were determined in *N*,*N*-dimethylformamide (Inskeep and Bloom, 1985) using fresh leaf discs (9 mm diameter).

Relative chlorophyll amount and chl *a*/*b* ratio values were measured from blue-native gel bands after overnight methanol extraction, based on absorbance at 646.6 and 665.2 nm (for chlorophyll *b* and chlorophyll *a*, respectively).

2-D lpBN Electrophoresis

2-D lpBN gel electrophoresis of *n*-dodecyl β-D-maltoside-solubilized thylakoid membranes was carried out according to Järvi et al. (2011). SYPRO Ruby and ProQ Diamond staining was performed according to Invitrogen instructions. Gel images were acquired by the Geliance 1000 Imaging System (Perkin-Elmer). Spot densitometry was performed by ProFinder 2D, version 2005 (Nonlinear Dynamics). The intensity value of every spot in ProQ- and SYPRO-stained gels was normalized based on the total intensity of all spots in the sample.

SDS-PAGE and Immunoblotting

For isolation of total foliar extracts, leaves were immediately frozen in liquid nitrogen, homogenized in ice-cold buffer (50 mM HEPES-KOH, pH 7.5, 100 mM sorbitol, 10 mM $MgCl_2$, and 20 mM NaF), and filtrated through Miracloth. Chlorophyll content was determined as described (Porra et al., 1989), and samples were solubilized, separated by SDS-PAGE according to Laemmli (1970) using 15% polyacrylamide and 6 M urea on the separation gel, and finally transferred to an Immobilon-P membrane (Millipore; http://www.millipore.com). After blocking with 5% milk (www.bio-rad.com), proteins were immunodetected with antibodies raised against D1, CP43, PsaB, Lhcb2, Lhca1, Cyt f, NdhL, PGRL1, PGR5, PTOX, ATPβ, or RbcL. Anti-Cyt f antibodies were kindly provided by L. Zhang, anti-NdhL and anti-PGR5 antibodies by T. Shikanai, anti-PGRL1 antibodies by D. Leister, and anti-PTOX antibodies by M. Kuntz. All the other antibodies were purchased from Agrisera. Horseradish peroxidase-linked secondary antibody and Amersham ECL western blotting detection reagents (GE Healthcare; http://www.gehealthcare.com) were used for detection.

In Vivo Measurements of PSII and PSI Photosynthetic Parameters

Dual-PAM-100 (Heinz Walz) was used for the simultaneous measurement of PSII and PSI photosynthetic parameters, based on chlorophyll *a* fluorescence and P700 oxidation signal (depending on the A_{830}; Klughammer and Schreiber 2008), respectively. The measuring light (460-nm wavelength) intensity for fluorescence measurements was 5 μmol photons m^{-2} s^{-1}. Red actinic light (635-nm wavelength) was used at intensities of 56 and 632 μmol photons m^{-2} s^{-1} to mimic the LL and HL phases of FL. The relative Q_A redox state was measured as F'/F_m, where F' is the fluorescence yield under actinic light and F_m is the maximal fluorescence from a dark-adapted leaf during a SP (6,000 μmol photons m^{-2} s^{-1}, 300 ms). NPQ was measured as $(F_m - F_m')/F_m'$ (Bilger and Björkman, 1990), where F_m' is the maximal fluorescence yield from illuminated leaf during a SP (a SP was given every 30 s). The PSI redox state and Y (NA) were determined according to Klughammer and Schreiber, 1994, 2008).

The chlorophyll fluorescence parameter F'/F_m from intact leaves was determined also by JTS-10 spectrometer (BioLogic SAS) using a green actinic light (520-nm wavelength) of 67 and 590 μmol photons m^{-2} s^{-1} intensities and a 250-ms SP (7900 μmol photons m^{-2} s^{-1}) provided by green light-emitting diodes.

Changes of PSI and PSII photochemical yields ratio [Y(I)/Y(II)] were used to estimate the induction of cyclic electron flow (Harbinson and Foyer, 1991). The measurements of Y(I)/Y(II) were carried out by using Dual-PAM-100. Detached leaves were incubated in darkness for 15 min and subsequently illuminated by red actinic light (635-nm wavelength).

The F_0 rise was detected in intact leaves after 5 min of illumination under white actinic light (100 μmol photons m^{-2} s^{-1}). The fluorescence signal was normalized to the F_m value.

For all the chlorophyll *a* fluorescence experiments, leaves were incubated in darkness for 15 min and a SP was applied before turning on the actinic light. Leaves from a minimum of three different plants of each mutant and the wild type were analyzed.

The $\Delta P/P_m$ and P_m parameters were measured based on changes of P700 redox state measured according to Dual-PAM-100 instructions (Klughammer and Schreiber, 1994, 2008). Leaf discs (9 mm diameter) collected from light-adapted plants were incubated in darkness for 5 min and illuminated by far-red light (720-nm wavelength, 191 μmol photons m^{-2} s^{-1}) for 9 s. On top of the far-red light, a SP (10,000 μmol photons m^{-2} s^{-1}, 300 ms) was applied, and

then both lights were turned off simultaneously. The differences between the signal upon a SP and darkness, and the signal upon a SP and the far-red light steady-state level, were denoted as P_m and ΔP, respectively (Supplemental Fig. S5). P_m values were normalized based on the leaf disc chlorophyll content (P_m μg^{-1} chlorophyll), determined after solubilization in *N*,*N*-dimethylformamide. It is worth noting that the P_m μg^{-1} chlorophyll parameter underestimates the differences in PSI amount between samples, mainly because of the scattering of light passing through the leaf. Since wild-type and *stn7* plants showed similar leaf morphology and chlorophyll concentration per area, we maintain that this technical limitation constituted a systematic error that cannot account for the observed linear correlations.

The 77 K chlorophyll *a* fluorescence emission spectra were recorded (Murata et al., 1966). Thylakoids were isolated and diluted in buffer containing 50 mM HEPES/KOH, pH 7.5, 100 mM sorbitol, 10 mM $MgCl_2$, and 10 mM NaF to a chlorophyll concentration of 10 μg mL^{-1} and subjected to measurements of 77 K chlorophyll *a* fluorescence emission spectra using a diode array spectrophotometer (S2000; Ocean Optics) equipped with a reflectance probe. To record the 77 K fluorescence emission curves, the samples were excited with blue light (wavelengths below 500 nm; derived from white light filtered by LS500S and LS700S filters [Corion]). The emission between 600 and 800 nm was recorded and normalized according to the value at 685 nm.

Supplemental Data

The following materials are available in the online version of this article.

Supplemental Figure S1. Rosette diameter (relative values) of Arabidopsis wild-type and mutant plants grown under constant light and FL.

Supplemental Figure S2. The chl *a/b* ratio and distribution of chlorophyll between pigment-protein complexes in wild-type and *stn7* mutant plants grown under ML and FL conditions.

Supplemental Figure S3. The 77K chlorophyll *a* fluorescence spectra of wild-type and *stn7* mutant plants grown in constant LL, ML, and HL growth conditions and under FL, and wild-type and *stn7* PSII/PSI emission peak ratios.

Supplemental Figure S4. Visual phenotype and relative Q_A reduction (chlorophyll *a* fluorescence parameter F'/F_m) in wild-type and *psal* mutant plants grown under FL.

Supplemental Figure S5. Supplemental information on data shown in Figure 6.

Supplemental Figure S6. Cyclic electron flow around PSI in wild-type and *stn7* plants grown under ML and FL conditions.

Supplemental Figure S7. Amount of PSI and intersystem ETC reduction, plotted against chl *a/b* ratio, in wild-type and *stn7* mutant plants grown under LL and HL.

Supplemental Figure S8. Schematic model of the redox state of the ETC (PQ and PC) and the reducing side of PSI (stroma) in wild-type and *stn7* plants under LL and HL.

ACKNOWLEDGMENTS

Ilaf Shorrsh Bilal, Maija Holmström, and Anniina Leppäniemi are acknowledged for their help in immunoblot and 2-D lpBN-PAGE experiments, and Marjaana Suorsa and Esa Tyystjärvi for fruitful discussions.

Received August 29, 2012; accepted September 27, 2012; published October 2, 2012.

LITERATURE CITED

Allen JF (2003) State transitions: a question of balance. Science **299:** 1530–1532

Aro EM, Suorsa M, Rokka A, Allahverdiyeva Y, Paakkarinen V, Saleem A, Battchikova N, Rintamäki E (2005) Dynamics of photosystem II: a proteomic approach to thylakoid protein complexes. J Exp Bot **56:** 347–356

Bailey S, Horton P, Walters RG (2004) Acclimation of Arabidopsis thaliana to the light environment: the relationship between photosynthetic function and chloroplast composition. Planta **218:** 793–802

Bailey S, Walters RG, Jansson S, Horton P (2001) Acclimation of Arabidopsis thaliana to the light environment: the existence of separate low light and high light responses. Planta **213:** 794–801

Barros T, Kühlbrandt W (2009) Crystallisation, structure and function of plant light-harvesting complex II. Biochim Biophys Acta **1787:** 753–772

Bellafiore S, Barneche F, Peltier G, Rochaix JD (2005) State transitions and light adaptation require chloroplast thylakoid protein kinase STN7. Nature **433:** 892–895

Bendall D (1982) Photosynthetic cytochromes of oxygenic organisms. Biochim Biophys Acta **683:** 119–151

Bilger W, Björkman O (1990) Role of the xanthophyll cycle in photoprotection elucidated by measurements of light-induced absorbency changes, fluorescence and photosynthesis in leaves of Hedera canariensis. Photosynth Res **25:** 173–185

Bonardi V, Pesaresi P, Becker T, Schleiff E, Wagner R, Pfannschmidt T, Jahns P, Leister D (2005) Photosystem II core phosphorylation and photosynthetic acclimation require two different protein kinases. Nature **437:** 1179–1182

Canaani O, Malkin S (1984) Distribution of light excitation in an intact leaf between the 2 photosystems of photosynthesis: changes in absorption cross-sections following state 1-state 2 transitions. Biochim Biophys Acta **766:** 513–524

de Bianchi S, Ballottari M, Dall'osto L, Bassi R (2010) Regulation of plant light harvesting by thermal dissipation of excess energy. Biochem Soc Trans **38:** 651–660

Demmig-Adams B, Adams WW III (2006) Photoprotection in an ecological context: the remarkable complexity of thermal energy dissipation. New Phytol **172:** 11–21

Dietz K, Schreiber U, Heber U (1985) The relationship between the redox state of Qa and photosynthesis in leaves at various carbon-dioxide, oxygen and light regimes. Planta **166:** 219–226

Dietzel L, Bräutigam K, Pfannschmidt T (2008) Photosynthetic acclimation: state transitions and adjustment of photosystem stoichiometry. Functional relationships between short-term and long-term light quality acclimation in plants. FEBS J **275:** 1080–1088

Eberhard S, Finazzi G, Wollman FA (2008) The dynamics of photosynthesis. Annu Rev Genet **42:** 463–515

Fernández AP, Strand A (2008) Retrograde signaling and plant stress: plastid signals initiate cellular stress responses. Curr Opin Plant Biol **11:** 509–513

Fernyhough P, Foyer C, Horton P (1983) The influence of metabolic state on the level of phosphorylation of the light-harvesting chlorophyll-protein complex in chloroplasts isolated from maize mesophyll. Biochim Biophys Acta **725:** 155–161

Fork D, Satoh K (1986) The control by state transitions of the distribution of excitation-energy in photosynthesis. Annu Rev Plant Physiol Plant Mol Biol **37:** 335–361

Foyer C, Furbank R, Harbinson J, Horton P (1990) The mechanisms contributing to photosynthetic control of electron-transport by carbon assimilation in leaves. Photosynth Res **25:** 83–100

Foyer CH, Neukermans J, Queval G, Noctor G, Harbinson J (2012) Photosynthetic control of electron transport and the regulation of gene expression. J Exp Bot **63:** 1637–1661

Frenkel M, Bellafiore S, Rochaix J, Jansson S (2007) Hierarchy amongst photosynthetic acclimation responses for plant fitness. Physiol Plant **129:** 455–459

Gray GR, Savitch LV, Ivanov AG, Hüner NPA (1996) Photosystem II excitation pressure and development of resistance to photoinhibition. 2. Adjustment of photosynthetic capacity in winter wheat and winter rye. Plant Physiol **110:** 61–71

Haldrup A, Jensen PE, Lunde C, Scheller HV (2001) Balance of power: a view of the mechanism of photosynthetic state transitions. Trends Plant Sci **6:** 301–305

Harbinson J, Foyer CH (1991) Relationships between the efficiencies of photosystems I and II and stromal redox state in CO_2-free air: evidence for cyclic electron flow in vivo. Plant Physiol **97:** 41–49

Hope AB (1993) The chloroplast cytochrome bf complex: a critical focus on function. Biochim Biophys Acta **1143:** 1–22

Horton P, Ruban A (2005) Molecular design of the photosystem II light-harvesting antenna: photosynthesis and photoprotection. J Exp Bot **56:** 365–373

Hou CX, Rintamäki E, Aro EM (2003) Ascorbate-mediated LHCII protein phosphorylation: LHCII kinase regulation in light and in darkness. Biochemistry **42:** 5828–5836

Hüner N, Maxwell D, Gray G, Savitch L, Krol M, Ivanov A, Falk S (1996) Sensing environmental temperature change through imbalances between energy supply and energy consumption: redox state of photosystem II. Physiol Plant **98:** 358–364

Inskeep WP, Bloom PR (1985) Extinction coefficients of chlorophyll *a* and chlorophyll *b* in *N*,*N*-dimethylformamide and 80% acetone. Plant Physiol **77:** 483–485

Jahns P, Holzwarth AR (2012) The role of the xanthophyll cycle and of lutein in photoprotection of photosystem II. Biochim Biophys Acta **1817:** 182–193

Järvi S, Suorsa M, Paakkarinen V, Aro EM (2011) Optimized native gel systems for separation of thylakoid protein complexes: novel super- and mega-complexes. Biochem J **439:** 207–214

Joliot A, Joliot P (1964) Etude cinetique de la reaction photochimique liberant loxygene au cours de la photosynthese. C R Hebd Seances Acad Sci **258:** 4622–4625

Joliot P, Johnson GN (2011) Regulation of cyclic and linear electron flow in higher plants. Proc Natl Acad Sci USA **108:** 13317–13322

Kargul J, Barber J (2008) Photosynthetic acclimation: structural reorganisation of light harvesting antenna. Role of redox-dependent phosphorylation of major and minor chlorophyll a/b binding proteins. FEBS J **275:** 1056–1068

Klughammer C, Schreiber U (1994) An improved method, using saturating light-pulses, for the determination of photosystem I quantum yield via $P700^+$-absorbency changes at 830 nm. Planta **192:** 261–268

Klughammer C, Schreiber U (2008) PAM Application Notes (PAN) **1:** 11–14. http://www.walz.com (August 29, 2012)

Kramer DM, Johnson G, Kiirats O, Edwards GE (2004) New fluorescence parameters for the determination of Q(a) redox state and excitation energy fluxes. Photosynth Res **79:** 209–218

Külheim C, Agren J, Jansson S (2002) Rapid regulation of light harvesting and plant fitness in the field. Science **297:** 91–93

Laemmli UK (1970) Cleavage of structural proteins during the assembly of the head of bacteriophage T4. Nature **227:** 680–685

Lavergne J, Trissl HW (1995) Theory of fluorescence induction in photosystem II: derivation of analytical expressions in a model including exciton-radical-pair equilibrium and restricted energy transfer between photosynthetic units. Biophys J **68:** 2474–2492

Lemeille S, Turkina MV, Vener AV, Rochaix JD (2010) Stt7-dependent phosphorylation during state transitions in the green alga Chlamydomonas reinhardtii. Mol Cell Proteomics **9:** 1281–1295

Lemeille S, Willig A, Depège-Fargeix N, Delessert C, Bassi R, Rochaix JD (2009) Analysis of the chloroplast protein kinase Stt7 during state transitions. PLoS Biol **7:** 644–675

Leong TY, Anderson JM (1984) Adaptation of the thylakoid membranes of pea chloroplasts to light intensities. 1. Study on the distribution of chlorophyll-protein complexes. Photosynth Res **5:** 105–115

Lunde C, Jensen PE, Haldrup A, Knoetzel J, Scheller HV (2000) The PSI-H subunit of photosystem I is essential for state transitions in plant photosynthesis. Nature **408:** 613–615

Malkin S, Telfer A, Barber J (1986) Quantitative-analysis of state-1 state-2 transitions in intact leaves using modulated fluorometry: evidence for changes in the absorption cross-section of the 2 photosystems during state transitions. Biochim Biophys Acta **848:** 48–57

Minagawa J (2011) State transitions: the molecular remodeling of photosynthetic supercomplexes that controls energy flow in the chloroplast. Biochim Biophys Acta **1807:** 897–905

Miyake C, Amako K, Shiraishi N, Sugimoto T (2009) Acclimation of tobacco leaves to high light intensity drives the plastoquinone oxidation system: relationship among the fraction of open PSII centers, non-photochemical quenching of Chl fluorescence and the maximum quantum yield of PSII in the dark. Plant Cell Physiol **50:** 730–743

Murata N (2009) The discovery of state transitions in photosynthesis 40 years ago. Photosynth Res **99:** 155–160

Murata N, Nishimura M, Takamiya A (1966) Fluorescence of chlorophyll in photosynthetic systems. 3. Emission and action spectra of fluorescence: three emission bands of chlorophyll a and the energy transfer between two pigment systems. Biochim Biophys Acta **126:** 234–243

Nishio JN, Whitmarsh J (1993) Dissipation of the proton electrochemical potential in intact chloroplasts. II. The pH gradient monitored by cytochrome f reduction kinetics. Plant Physiol **101:** 89–96

Niyogi KK (1999) Photoprotection revisited: genetic and molecular approaches. Annu Rev Plant Physiol Plant Mol Biol **50:** 333–359

Niyogi KK, Grossman AR, Björkman O (1998) *Arabidopsis* mutants define a central role for the xanthophyll cycle in the regulation of photosynthetic energy conversion. Plant Cell **10:** 1121–1134

Niyogi KK, Li XP, Rosenberg V, Jung HS (2005) Is PsbS the site of non-photochemical quenching in photosynthesis? J Exp Bot **56:** 375–382

Pfannschmidt T, Nilsson A, Allen JF (1999) Photosynthetic control of chloroplast gene expression. Nature **397:** 625–628

Piippo M, Allahverdiyeva Y, Paakkarinen V, Suoranta UM, Battchikova N, Aro EM (2006) Chloroplast-mediated regulation of nuclear genes in Arabidopsis thaliana in the absence of light stress. Physiol Genomics **25:** 142–152

Porra RJ, Thompson WA, Kriedemann PE (1989) Determination of accurate extinction coefficients and simultaneous equations for assaying chlorophyll a and chlorophyll b extracted with 4 different solvents: verification of the concentration of chlorophyll standards by atomic absorption spectroscopy. Biochim Biophys Acta **975:** 384–394

Pribil M, Pesaresi P, Hertle A, Barbato R, Leister D (2010) Role of plastid protein phosphatase TAP38 in LHCII dephosphorylation and thylakoid electron flow. PLoS Biol **8:** e1000288

Rintamäki E, Martinsuo P, Pursiheimo S, Aro EM (2000) Cooperative regulation of light-harvesting complex II phosphorylation via the plastoquinol and ferredoxin-thioredoxin system in chloroplasts. Proc Natl Acad Sci USA **97:** 11644–11649

Rintamäki E, Salonen M, Suoranta UM, Carlberg I, Andersson B, Aro EM (1997) Phosphorylation of light-harvesting complex II and photosystem II core proteins shows different irradiance-dependent regulation in vivo: application of phosphothreonine antibodies to analysis of thylakoid phosphoproteins. J Biol Chem **272:** 30476–30482

Rochaix JD (2007) Role of thylakoid protein kinases in photosynthetic acclimation. FEBS Lett **581:** 2768–2775

Ruban AV, Johnson MP (2009) Dynamics of higher plant photosystem cross-section associated with state transitions. Photosynth Res **99:** 173–183

Ruban AV, Johnson MP, Duffy CD (2012) The photoprotective molecular switch in the photosystem II antenna. Biochim Biophys Acta **1817:** 167–181

Rumberg B, Siggel U (1969) pH changes in the inner phase of the thylakoids during photosynthesis. Naturwissenschaften **56:** 130–132

Shapiguzov A, Ingelsson B, Samol I, Andres C, Kessler F, Rochaix JD, Vener AV, Goldschmidt-Clermont M (2010) The PPH1 phosphatase is specifically involved in LHCII dephosphorylation and state transitions in Arabidopsis. Proc Natl Acad Sci USA **107:** 4782–4787

Smith H (1982) Light quality, photoperception, and plant strategy. Annu Rev Plant Physiol Plant Mol Biol **33:** 481–518

Sonoike K, Terashima I, Iwaki M, Itoh S (1995) Destruction of photosystem I iron-sulfur centers in leaves of Cucumis sativus L. by weak illumination at chilling temperatures. FEBS Lett **362:** 235–238

Suorsa M, Järvi S, Grieco M, Nurmi M, Pietrzykowska M, Rantala M, Kangasjärvi S, Paakkarinen V, Tikkanen M, Jansson S, et al (2012) PROTON GRADIENT REGULATION5 is essential for proper acclimation of *Arabidopsis* photosystem I to naturally and artificially fluctuating light conditions. Plant Cell **24:** 2934–2948

Tikhonov A, Khomutov G, Ruuge E, Blumenfeld L (1981) Electron-transport control in chloroplasts: effects of photosynthetic control monitored by the intrathylakoid pH. Biochim Biophys Acta **637:** 321–333

Tikkanen M, Grieco M, Aro EM (2011) Novel insights into plant light-harvesting complex II phosphorylation and 'state transitions.' Trends Plant Sci **16:** 126–131

Tikkanen M, Grieco M, Kangasjärvi S, Aro EM (2010) Thylakoid protein phosphorylation in higher plant chloroplasts optimizes electron transfer under fluctuating light. Plant Physiol **152:** 723–735

Tikkanen M, Nurmi M, Kangasjärvi S, Aro EM (2008a) Core protein phosphorylation facilitates the repair of photodamaged photosystem II at high light. Biochim Biophys Acta **1777:** 1432–1437

Tikkanen M, Nurmi M, Suorsa M, Danielsson R, Mamedov F, Styring S, Aro EM (2008b) Phosphorylation-dependent regulation of excitation energy distribution between the two photosystems in higher plants. Biochim Biophys Acta **1777:** 425–432

Tikkanen M, Piippo M, Suorsa M, Sirpiö S, Mulo P, Vainonen J, Vener AV, Allahverdiyeva Y, Aro EM (2006) State transitions revisited: a buffering system for dynamic low light acclimation of Arabidopsis. Plant Mol Biol **62:** 779–793

Tullberg A, Alexciev K, Pfannschmidt T, Allen JF (2000) Photosynthetic electron flow regulates transcription of the psaB gene in pea (Pisum sativum L.) chloroplasts through the redox state of the plastoquinone pool. Plant Cell Physiol **41:** 1045–1054

Vainonen JP, Hansson M, Vener AV (2005) STN8 protein kinase in Arabidopsis thaliana is specific in phosphorylation of photosystem II core proteins. J Biol Chem **280:** 33679–33686

Walters RG (2005) Towards an understanding of photosynthetic acclimation. J Exp Bot **56:** 435–447

Weis E, Berry J (1987) Quantum efficiency of photosystem II in relation to energy-dependent quenching of chlorophyll fluorescence. Biochim Biophys Acta **894:** 198–208

Williams W, Allen J (1987) State-1/state-2 changes in higher plants and algae. Photosynth Res **13:** 19–45

Witt HT (1979) Energy conversion in the functional membrane of photosynthesis: analysis by light pulse and electric pulse methods. The central role of the electric field. Biochim Biophys Acta **505:** 355–427

Wollman FA (2001) State transitions reveal the dynamics and flexibility of the photosynthetic apparatus. EMBO J **20:** 3623–3630

Yang DH, Webster J, Adam Z, Lindahl M, Andersson B (1998) Induction of acclimative proteolysis of the light-harvesting chlorophyll *a/b* protein of photosystem II in response to elevated light intensities. Plant Physiol **118:** 827–834